Assessing streamflow sensitivity to precipitation variability in karst-influenced catchments with unclosed water balance

Yan Liu[1], Thorsten Wagener[2, 3], and Andreas Hartmann[1, 2]

[1]Chair of Hydrological Modeling and Water Resources, University of Freiburg, 79098 Freiburg, Germany
[2]Department of Civil Engineering, University of Bristol, Bristol, UK
[3]Cabot Institute, University of Bristol, Bristol, UK

Correspondence to: Yan Liu (yan.liu@hydmod.uni-freiburg.de)

Key Points:

- We present a combined model approach for karst-influenced catchments with unclosed water balance.
- We investigate the karstic and non-karstic contributions to streamflow sensitivity at six test catchments across Europe and Middle East.
- We find that inter-catchment groundwater flow modifies the importance of karst to the total streamflow sensitivity.

Abstract

Karst hydrological models are widely used for simulating groundwater dynamics at the aquifer scale. However, modeling streamflow of a topographic catchment that is partially covered by karst is rarely reported. This is due to difficulties of properly considering the strong differences of karstic and non-karstic hydrodynamics and the widespread occurrence of unclosed water balances in karstic regions caused by inter-catchment groundwater flow. In this study, we present a new approach that uses hydrologic signatures to identify important processes and appropriate model structures for the simulation of karst-influenced catchments. We include a new method that accounts for karstic inter-catchment groundwater flow. We apply our approach to six karst-influenced test catchments in Europe and Middle

East. We estimate the contributions of karstic and non-karstic parts to total streamflow sensitivity. With different model structures identified at different sites, our simulation approach provides acceptable simulations especially at those catchments where inter-catchment groundwater flow is deemed important. Using the models to calculate the streamflow sensitivity to precipitation variability, we find that inter-catchment groundwater flow reduces the contribution of karstic area to the total streamflow sensitivity for the losing catchments, while increases that for the gaining catchments. Modeling streamflow at karst-influenced catchments requires the consideration of differences between karst and non-karst, and inter-catchment groundwater flow matters for catchments with unclosed water balance.

1 Introduction

Karst water resources are estimated to provide drinking water to 10%−25% of the world's population (Ford & Williams, 2007; Stevanović, 2019). In some countries and regions, e.g., Austria and Slovenia, the karst water accounts for approximately half of the total water supply (Hartmann et al., 2014; Stevanović, 2019). Chemical weathering of the carbonate rock results in a strong subsurface heterogeneity at karstic areas, which can lead to groundwater recharge and storage behavior substantially different from the non-karstic regions (Bakalowicz, 2005; Hartmann & Baker, 2017). Climate projections suggest strong changes of temperature and precipitation in almost all karstic regions in the world (Christensen et al., 2007) affecting their hydrological dynamics and water availability by unknown extent. New approaches to understanding the impact of climate change at karstic regions is therefore of great importance.

Recent achievements in karst research include the creation of karst spring discharge databases to promote data availability at karstic regions (Olarinoye et al., 2020), relating soil moisture networks to karst groundwater storage and flow (Berthelin et al., 2020), using tracer experiments to detect fast and slow pathways and the connectivity of conduit systems (Lüthi, 2019; Morales et al., 2007; Perrin & Luetscher, 2008), investigating contaminant transport and vulnerability of karst systems (Butscher et al., 2011; Mudarra et al., 2019; Pinault et al., 2001), and modeling recharge and discharge time-series (Gunkel et al., 2015; Jourde et al., 2014; Reimann et al., 2011; Smiatek et al., 2012). The majority of these studies looks

at the aquifer scale and therefore focuses on groundwater discharge at the karst springs. The recharge area of the aquifer is commonly considered as the most appropriate spatial unit for their characterization and for model applications.

In catchment hydrology, topographically delineated catchments represent the common units for studies at catchment scale, e.g., hydrological simulations of the catchment responses (Clark et al., 2017; Kirchner, 2009), drought and flood analyses (Haslinger et al., 2014; Merz & Blöschl, 2005; Tallaksen et al., 2009), sediment production and transport from hillslopes to rivers (Liu et al., 2018; Sherriff et al., 2016; Zuo et al., 2016), and the behavior and fate of nutrients and pollutants (Liu et al., 2019; Van Meter & Basu, 2017; Pullan et al., 2016). However, previous work showed that the water balance of topographic catchments may often not be closed (Fan, 2019; Liu et al., 2020; Le Mesnil et al., 2020). This is particularly true for karstic regions where recharge areas are often found to not be equal to the topographic catchment. The strong differences of karstic and non-karstic hydrological processes make the consideration of karst aquifers in the catchment-scale simulation additionally challenging.

Only few simulation studies (Chen et al., 2018; Rimmer & Salingar, 2006) have jointly considered karstic and non-karstic processes at the catchment scale. They found that modeling discharge of karst-influenced catchment needs to consider separate surface and subsurface drainage domains, as well as different hydrodynamics for karstic and non-karstic simulation domains. Both studies used conceptual simulation models for a site-specific purpose. To our knowledge, no generally applicable approach to simulate karst-influenced catchments with unclosed water balance is yet available. Signatures, inferring a system's hydrologic behavior (Wagener et al., 2007), have been used for characterization of hydrologic changes (Sawicz et al., 2014) and particularly for in-depth model calibration and evaluation (Gunkel et al., 2015; Hingray et al., 2010). They also helped to systematically derive conceptual understandings about important hydrologic processes in karstic regions (Hartmann, et al., 2013) and may therefore offer a promising direction for identifying important hydrologic processes and model structures in karst-influenced catchments.

In this study, we present a new simulation approach that identifies karstic and non-karstic processes at the catchment scale using signatures and translates them into site-specific model structures. To elaborate the applicability of our new approach, we select six test catchments that are composed of karstic and non-karstic areas at different climates and with varying degrees of karst coverage in Europe and Middle East. We evaluate our simulations with traditional performance measures and the signatures. We finally use the evaluated model structures to assess the sensitivity of total streamflow to precipitation changes and the contribution of each catchment's karstic and non-karstic areas to the total streamflow sensitivity.

2 Materials and Methods

We use a combination of established signatures and a newly defined karst-specific signature to identify important processes and model structures at a set of karst-influenced catchments with unclosed water balance. Looking at catchments with varying influence of karst and using a wide range of performance measures and signatures, we can assess the robustness of our new approach and use the models to investigate the sensitivity of discharge to the climate variability for both karstic and non-karstic parts.

2.1 Conceptualization of system processes

2.1.1 Signatures to identify important processes

Signatures are helpful to systematically characterize the behavior of a hydrologic system (Sawicz et al., 2011; Jothityangkoon et al., 2001; McMillan, 2020). For the conceptualization of a karst-influenced hydro-system, as discussed in the introduction, we have to solve problems of inter-catchment groundwater flow (IGF) that result in differences between topographic and subsurface domains while having to address the general questions of how to represent snow and channel processes. For that purpose, we use established signatures and a newly-defined karst-specific signature (table 1) to identify the important processes for the karst-influenced catchments using the following rules:

(1) Is the snow process important?

Snowfall fraction (R_{sp}) measures how much precipitation falling as snowfall and therefore determines the importance of the snow process. McMillan et al (2018) showed that the typical magnitude of uncertainty in the precipitation measurement is about 10%. If $R_{sp} \leq 10\%$, the snow effect is in range of the precipitation uncertainty. However, if $R_{sp} > 10\%$, the snow process would become more important.

(2) Is the channel process important?

Channel length (L_c) controls the travel time of water from upstream to the downstream gauging point. If considering a variable storage of the channel routing for simplification (Kim & Lee, 2010; Williams, 1969), the outflow of the channel is only dependent from the inflow when the travel time in the channel is smaller than half of the temporal resolution of the model. Therefore, at the daily resolution we take the distance that water travels over half a day as the threshold to indicate the importance of the channel process, i.e., $L_c \geq 43.2$ km by assuming 1 m s^{-1} of flow velocity.

(3) Is the karstic process accounting for IGF important?

If the long-term mean of the effective catchment index (ECI, Liu et al., 2020) is not zero and all the inter-annual ECI values show the effective catchment area towards one direction, either all smaller or all larger than the topographic catchment, the karstic process accounting for IGF would be important. In addition, runoff ratio $R_{qp} > 1$ is another indicator.

Table 1. Signatures that are used to identify important processes, to evaluate the model simulations, and to indicate the streamflow sensitivity.

Signature	Symbol	Equation	Description	Purpose	Reference
Snowfall fraction	R_{sp} [-]	$R_{sp} = \frac{P_{snow}}{P}$	Characterizes the general significance of snow storage	System identification: Snow process	(Sawicz et al., 2011)
Channel length	L_c [km]	–	Characterizes the travel time of streamflow in the river channel	System identification: Channel process	–
Runoff ratio	R_{qp} [-]	$R_{qp} = \frac{Q}{P}$	Characterizes the catchment water balance: the separation of precipitation to streamflow and evapotranspiration	System identification: IGF & model evaluation	(Sawicz et al., 2011)
Effective catchment index	ECI [-]	$ECI = \log\left(\frac{Q}{P - AET}\right)$	Characterizes groundwater gains or losses of a topographic catchment by the karstic system	System identification: IGF	(Liu et al., 2020)
Slope of flow duration curve	S_{fdc} [-]	$S_{fdc} = \frac{\ln(Q_{33\%}) - \ln(Q_{66\%})}{0.66 - 0.33}$	Characterizes the flow variability	Model evaluation	(Yadav et al., 2007)
Streamflow elasticity	E_{QP} [-]	$E_{QP} = \text{median}\left(\frac{dQ}{dP}\frac{P}{Q}\right)$	Characterizes the sensitivity of a catchment's streamflow response to changes in precipitation at the annual time scale.	Streamflow sensitivity	(Sankarasubramanian et al., 2001)

P [mm d^{-1}] and P_{snow} [mm d^{-1}] are the long-term average of the total precipitation and the long-term average of snowfall (precipitation under temperature below 2 °C), respectively; AET [mm d^{-1}] and Q [mm d^{-1}] represent actual evapotranspiration and catchment-specific streamflow, respectively. $Q_{33\%}$ [mm d^{-1}] and $Q_{66\%}$ [mm d^{-1}] are the streamflow values at the 33rd and 66th percentile, respectively. To calculate ECI, the actual evapotranspiration of GLEAM (Global Land Evaporation Amsterdam Model: Martens et al., 2017; Miralles et al., 2011) is used, which is widely used and advanced global evapotranspiration product (Miralles et al., 2016).

2.1.2 Approach to combine karstic and non-karstic processes

We propose a new approach to take into account IGF and karst spring discharge such that we can combine karstic and non-karstic processes at the catchment scale. For a catchment composed of karstic and non-karstic areas, the likely contribution of the karstic part to IGF is considerably high. We show the concept of considering IGF to combine karstic and non-karstic processes in Fig. 1. First, we use a karstic

model to determine the recharge area of karst springs and obtain the karstic specific discharge. Second, using ECI defined in table 1, we can estimate the effective karstic area and make the effective catchment area as a parameter in the combined model (karstic + non-karstic models) to include IGF. Finally, we derive the total streamflow by summing up the karstic discharge (karstic specific discharge times effective karstic area) and non-karstic discharge (from the non-karstic model).

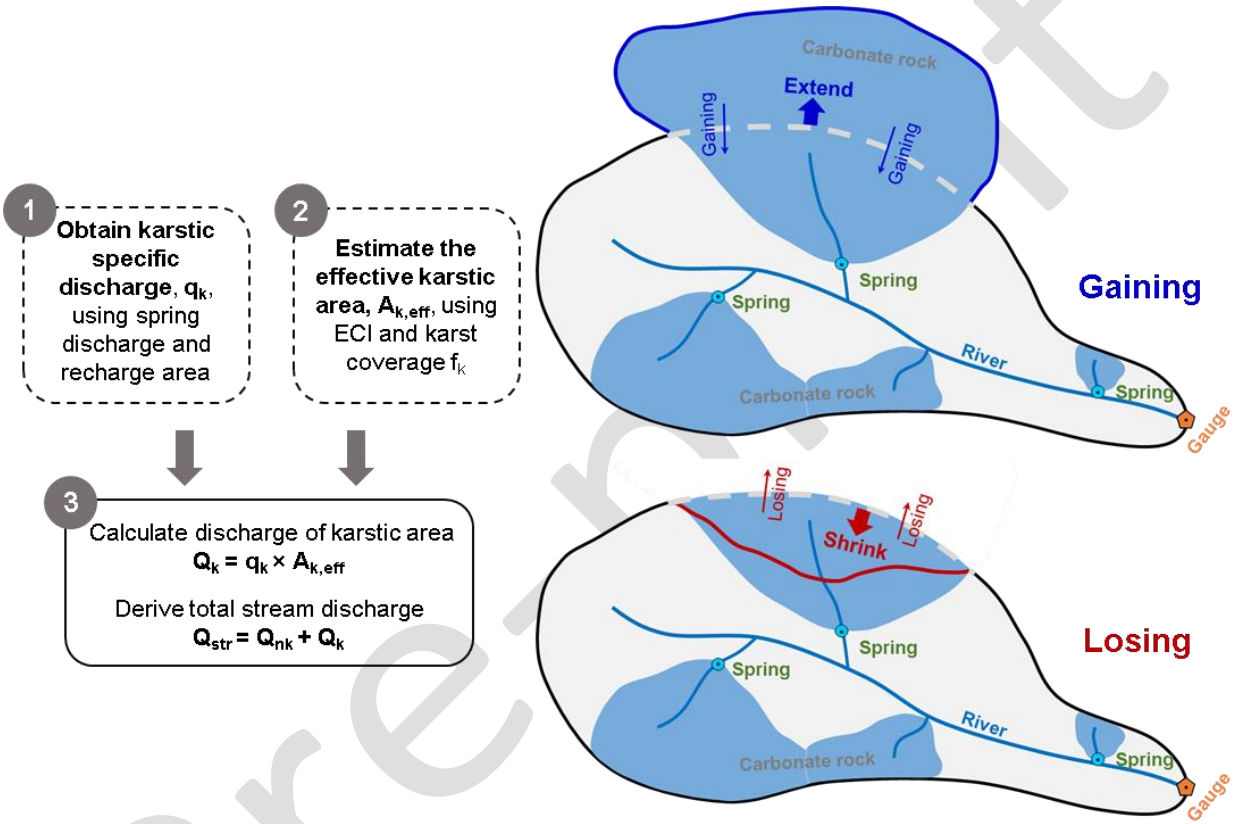

Figure 1. Concept of combining karstic and non-karstic processes with the consideration of IGF for water gaining and losing catchments.

2.2 Test catchments

2.2.1 Test catchment selection

The modeling approach is tested at six catchments, located in Austria (AT), Germany (DE), Spain (ES), France (FR), Ireland (IE), and Israel (IL). These sites (i) are composed of karstic and non-karstic areas with gauged rivers and karst springs within the topographic boundaries; (ii) most of them provide ≥10 years of forcing and discharge observations to capture the possible range of hydrologic processes; (iii)

cover latitudes between 36.5° N and 54° N (Fig. 2) in different climates and landscapes (table 2). The catchment sizes are from tens to several hundreds of square kilometers with the topographic karst coverage of 43.5%−92.5%. The mean annual precipitation is between 700 mm at French site and around 1400 mm at the Irish site. The annual mean stream discharge ranges from 0.3 m^3s^{-1} to 14.6 m^3s^{-1}. Details about the individual catchments are provided in table 2.

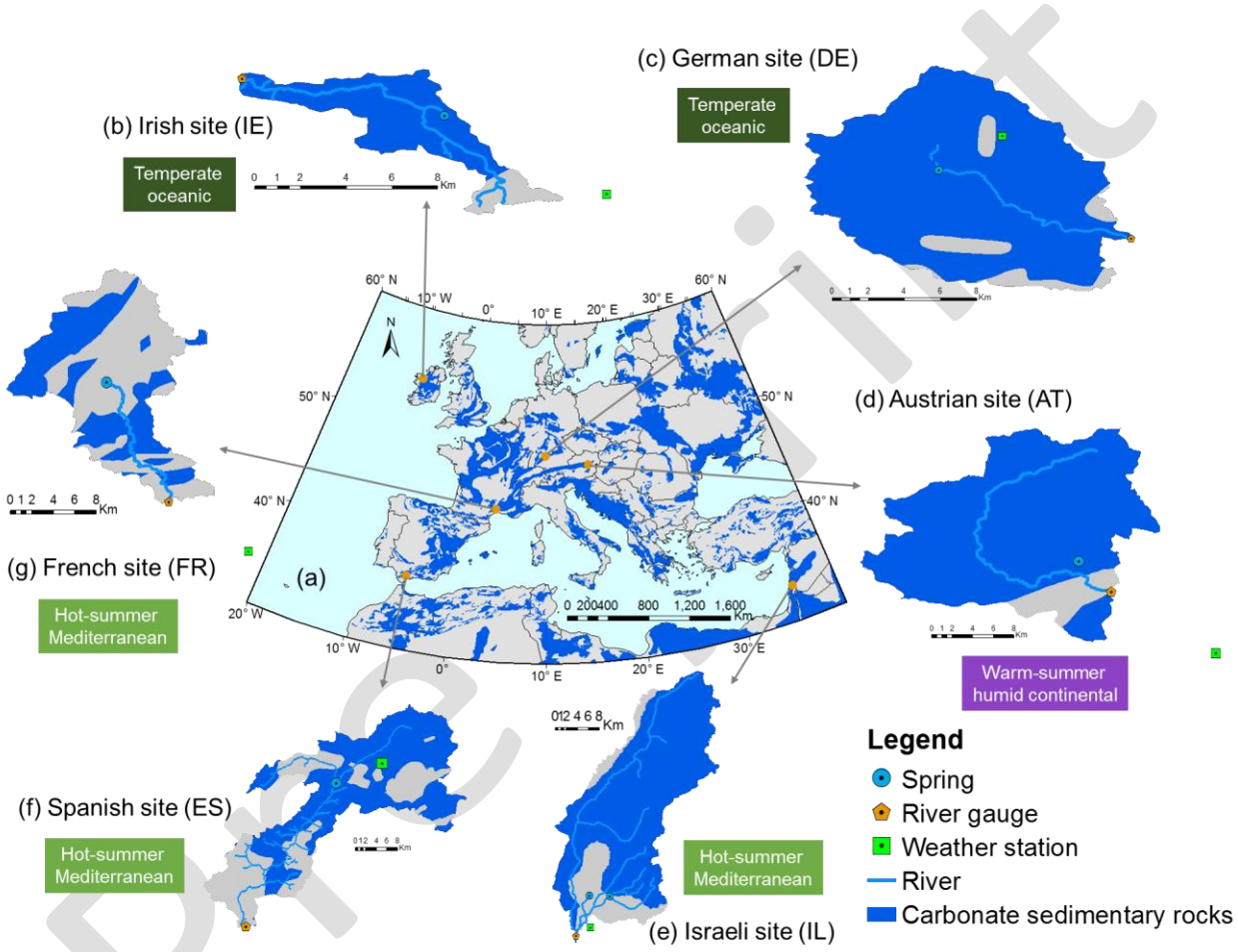

Figure 2. (a) Location of the study sites and (b)-(g) individual test catchments.

2.2.2 Available data

We have daily forcing data (precipitation and temperature), stream discharge observations from public observation databases, local meteorological and hydrological services, and publications (table 2 and table S4), and spring discharge observations from the World Karst Spring hydrograph database (WoKaS, Olarinoye et al., 2020). All discharge observations are available at daily resolution except for the Spanish

karst spring where observations are available every 6 days. Details about the data and sources are provided in table 2.

Table 2. Summary of catchment properties, forcing data, and discharge measurements for the six test catchments.

	Study sites	Austrian site (AT)	German site (DE)	Spanish site (ES)	French site (FR)	Irish site (IE)	Israeli site (IL)	
	Climate [a]	Dfb	Cfb	Csa	Csa	Cfb	Csa	
	Karst landscape type[b]	MTN	MTN	MED	HUM	HUM	MTN	
	Topographic catchment area (km^2)	231.5	107	603.8	150	18.3	783	
	Catchment boundary and rivers	HydroBASINS and HydroRIVERS of the HydroSHEDS (Lehner et al., 2008). Catchment boundaries are updated based on gauge locations and 25m EU-DEM of the Copernicus Land Monitoring Service (https://land.copernicus.eu/)					Hartmann et al., 2013	
	Karst coverage (%) [c]	92.5	92.2	61.7	43.5	84.9	81.5	
Forcing	Mean annual precipitation (mm)	1154.4	929.5	896.1	701.1	1381.7	901.1	
Forcing	Mean annual temperature (°C)	7.8	8.0	19.0	15.4	8.7	13.9	
Forcing	Source [d]	ZAMG	DWD	SAIH HIDROSUR	ECA&D	Met Éireann	Hartmann et al., 2013	
Stream	Name	Mürz	Lone	Guadiaro	Le Lez	Swinford	Jordan	
Stream	Q_{mean} (m^3s^{-1})	8.02	0.34	10.26	2.73	0.41	14.61	
Stream	Source [e]	eHYD	LUBW	SAIH HIDROSUR	HYDRO Eaufrance	Irish EPA	Hartmann et al., 2013	
Spring	Name	Siebenquellen	Lonetopf	Benaojan	Source du Lez	Killaturly	Dan	Banias
Spring	Q_{mean} (m^3s^{-1})	0.38	0.22	2.31	1.04	0.03	7.86	1.90
Spring	Source [f]	WoKaS						

[a] Csa: Hot-summer Mediterranean; Cfb: Temperate oceanic; Dfb: Warm-summer humid continental, which are based on the Köppen–Geiger climate classification.
[b] HUM: humid hills and plains; MTN High range mountains; MED: Mediterranean medium range mountains, according to Hartmann et al. (2015).
[c] WOKAM (World Karst Aquifer Map: Chen et al., 2017) and GLiM (Global Lithological Map: Hartmann et al., 2012) are used for the calculation of karst coverage.
[d,e,f] Details about the data source are provided in the table S4.

2.3 Model description

To represent the conceptual processes of the non-karstic and karstic systems, we choose two established hydrological models, i.e. HBV model (Lindström et al., 1997) and VarKarst model (Hartmann et al., 2013)

as the representatives for the non-karstic and karstic components, respectively. The HBV model represents typical catchment rainfall-runoff processes, while the VarKarst model represents a general conceptual model of karstic processes. A degree-day method is used to represent the snow routine (Lindström et al., 1997), and the Muskingum-Cunge method (Cunge, 1969) for the channel routing. Details of snow and channel processes are provided in the SI.

The HBV model has one soil water storage and two groundwater storages. Recharge from soil to the groundwater is partitioned by a function of the ratio between soil water storage and the maximum capacity. Flow from the two groundwater storage zones are computed by two linear outflow equations. Simulated flow dynamics of the HBV model are controlled by 8 parameters (table S2).

$$\frac{F(t)}{I(t)} = \left(\frac{SM(t)}{FC}\right)^{BETA} \quad (1)$$

$$Q_1 = k_1 S_{UZ} \quad (2)$$

$$Q_2 = k_2 S_{LZ} \quad (3)$$

where I(t) [mmd^{-1}] and F(t) [mmd^{-1}] are the amount of water input to the soil and the flux to the groundwater, respectively. SM(t) [mm] and FC [mm] are the current and maximum water storage in the soil box, respectively. BETA [−] is the shape coefficient of the recharge function. (Q_1 [mmd^{-1}], S_{UZ} [mm], k_1 [d^{-1}]) and (Q_2 [mmd^{-1}], S_{LZ} [mm], k_2 [d^{-1}]) are the discharge, storage, and recession coefficient of the upper and lower groundwater storage zones, respectively.

The VarKarst model considers the spatial heterogeneity using a distribution function that represents the spatial variability of subsurface properties such as the soil and epikarst storage capacities, or hydraulic conductivities. Running at a daily resolution, it simulates soil and epikarst storage dynamics, concentrated and diffuse recharge to the groundwater, and groundwater hydrodynamics, which are controlled by 8 model parameters (table S1).

$$S_{max,i} = S_{max,N}\left(\frac{i}{N}\right)^{a_{SE}} \quad (4)$$

$$K_{E,i} = K_{max,E}\left(\frac{N-i+1}{N}\right)^{a_{SE}} \quad (5)$$

$$K_{GW,i} = K_C\left(\frac{i}{N}\right)^{-a_{GW}} \quad (6)$$

where $S_{max,i}$ [mm] is the soil or epikarst storage capacity of model compartment i of N; $S_{max,N}$ [mm] is the overall maximum storage capacity of the soil or the epikarst; $K_{E,i}$ [d] and $K_{GW,i}$ [d] are the storage constants of the epikarst and groundwater at model compartment i; $K_{max,E}$ [d] is the overall maximum storage constant of the epikarst; K_C [d] is the conduit storage constant; a_{SE} [−] is dimensionless shape factors for soil and epikarst. a_{GW} [−] is dimensionless shape factors for groundwater.

2.4 Evaluation of the model structures

To test if our pre-selection of model structures (i) performs better for the discharge and signature simulations than a simple approach ignoring the karst characteristics, and (ii) is more robust than those considering certain or all possible processes, we benchmark them with alternative model structures (table 3). These include different combinations of karstic (K) and non-karstic (nK) model structures, as well as the (non-)consideration of snow (S) and channel routing (C). Benchmarking includes performance comparison and analysis of parameters sensitivities (see following subsection).

Table 3 model structures with different combinations of model processes at the catchment scale for the simulation of stream discharge.

Category	Non-karstic				Karstic + Non-karstic			
Model	nK	nK+C	nK+S	nK+C+S	nK+K	nK+K+C	nK+K+S	nK+K+C+S
Channel process	-	√	-	√	-	√	-	√
Snow process	-	-	√	√	-	-	√	√
Karstic process with IGF	-	-	-	-	√	√	√	√

2.5 Model calibration and evaluation

At all sites and for all models, we perform the model simulations at the daily resolution. Due to the data availability of spring and stream discharge observations, we use 15-year data for calibration and evaluation at all sites (8 years for calibration and 7 years for evaluation), except the Spanish site (ES),

where we only have 10-year data available (5 years for calibration and another 5 years for evaluation). Calibration and evaluation time periods are provided in table S5.

We use the differential evolution adaptive metropolis DREAM$_{(ZS)}$, a Markov Chain Monte Carlo algorithm, to calibrate our model parameters, which can efficiently estimate the posterior probability density function of model parameters (Liu et al., 2020; Vrugt, 2016) by minimizing the root mean squared error (RMSE). We warm up each model with a 5-year time loop of forcing data before the calibration period. The calibration ranges and descriptions of model parameters are provided in table S1-S3. To test their predictive skills, we apply our models with the calibrated parameter sets to the evaluation period for calculating changes using diagnostic objective functions. These include the volume conservation criteria (VCC), RMSE, and two of the previously defined signatures (the runoff ratio and the slope of flow duration curve; see table 1).

$$\mathrm{VCC} = \overline{Q_s}/\overline{Q_o}, \tag{7}$$

$$\mathrm{RMSE} = \sqrt{\frac{\sum_{i=1}^{n}\left(Q_{s,i}-Q_{o,i}\right)^2}{n}}, \tag{8}$$

where $\overline{Q_s}$ and $\overline{Q_o}$ represent the mean of the model simulations (Q_s) and observations (Q_o) of discharge, respectively. To explore if the results of our model calibrations are affected by parameter equifinality (Beven, 2006; Perrin et al., 2001; Kelleher et al., 2017), we analyze the shape of the posterior cumulative probability distributions of our model parameters obtained by DREAM$_{(ZS)}$. The more a parameter's posterior deviates from a uniform distribution, the more sensitive it is. If a large number of model parameters are sensitive, equifinality is most probably absent. We additionally test the robustness of our simulation with a split-sample test (Klemeš, 1986) that applies the parameter sets derived by DREAM$_{(ZS)}$ in the calibration period to the evaluation period.

2.6 Estimation of streamflow sensitivity

We use the streamflow elasticity (table 1) to quantify the streamflow sensitivity of a catchment due to the change of climate. In this study, we choose precipitation as the climate descriptor since it is the main driver of hydrologic systems. We calculate the elasticity for the total stream discharge as well as for the karstic and non-karstic specific discharge. We set two scenarios (traditional assumption of closed water balance at topographic catchments VS unclosed water balance to consider IGF) to compare the contribution of the karstic part to the total streamflow elasticity. For the closed water balance, the total elasticity is calculated using the elasticity of the specific discharges and their corresponding topographic area; while for the latter case, the total elasticity is calculated using the discharge simulations considering IGF with the karstic and non-karstic components.

3 Results

3.1 Model processes identified by historical data derived signatures

For the snow process (Fig. 3a), at the Austrian and German sites, the snowfall fraction regarding the inter-annual values and long-term mean are all larger than the threshold of 10%. It indicates that the snow process is potentially important for these two sites. At the Spanish, French, and Irish sites, the long-term mean of snow day ratio is much smaller than 10%, especially at Spanish and French sites the inter-annual values are all smaller than the threshold, such that the snow process may be unimportant for these three sites. At the Israeli site, the long-term mean of the snowfall fraction is below 10%, while the inter-annual values are partially larger than 10%. It suggests that the snow process may have influence on the hydrologic simulation at Israeli site, but the effect is not strong as Austrian and German sites.

For the channel process (Fig. 3b), only the stream at the Israeli site is longer than the half-day travel distance. It indicates that the water storage in the channel may influence the outflow at the catchment outlet at the daily resolution, which suggests that explicitly considering the channel process may be important. The channel length of the other five sites is much shorter than the threshold such that the explicit channel process is potentially not necessary, in particular under the daily resolution. Apart from

the channel length, the location and distribution of karst in the catchment may have influence that is not considered in this analysis.

For the karstic process with IGF (Fig. 3c-d), the long-term mean of runoff ratio at the Austrian site (Fig. 3c) is quite close to 1, and the inter-annual values even exceed 1, which indicates the water gains via IGF is potentially taking place. The positive ECI values of Austrian, Spanish, and French sites (Fig. 3d) suggest that the karstic process accounting for IGF is important to obtain the gaining water condition. The negative ECI values of German and Irish sites indicate the importance of considering IGF to represent the losing water condition. Whereas, at the Israeli site, the long-term mean of ECI is around zero, suggesting that IGF is not strong and unimportant.

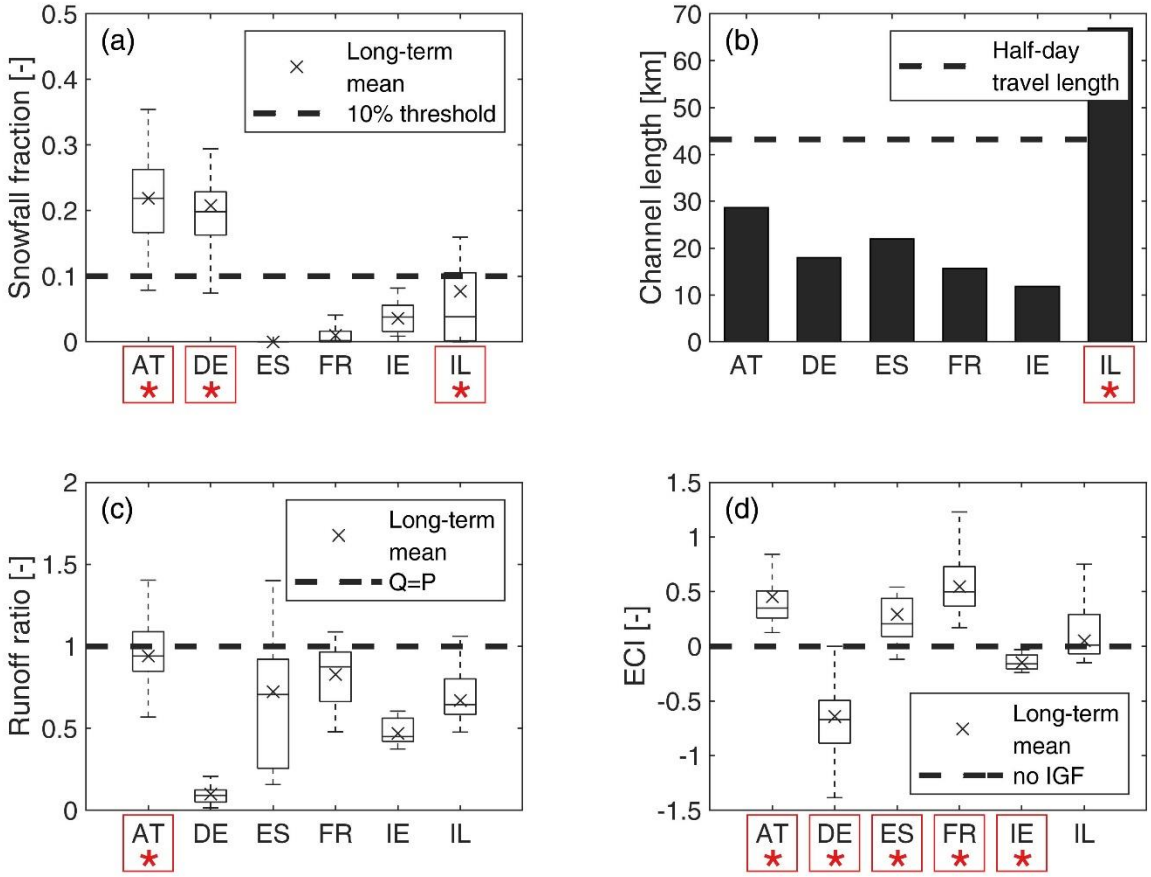

Figure 3. System signatures of the test catchments calculated from historical observations: (a) snowfall fraction; (b) channel length; (c) runoff ratio; and (d) effective catchment index (ECI). The boxplot shows the inter-annual variability; the cross (×) shows the signature calculated using the long-term mean of the historical observations; and dashed lines indicate the threshold. No IGF means no inter-catchment

groundwater flow. The red stars below the country code in each subplot indicate the important processes identified by signature for the marked sites.

3.2 Evaluation of model simulations

3.2.1 Model performance

Fig. 4 shows the comparison of stream discharge simulations using the non-karstic model approach against the signature-identified model structure (our new approach that combines the karstic and non-karstic areas to account for IGF). The German site exhibits the largest deviation between the two approaches. The ECI of the German site indicates a smaller subsurface area, which can be clearly reflected by the large overestimation of the base flow using the traditional non-karstic model without considering IGF (green line in Fig. 4 at DE). Using our combined model approach (orange line in Fig. 4 at DE), the low flow, peaks, and the recession of the hydrograph are simulated very well for both calibration and evaluation. At the Spanish and French sites, two approaches perform similarly for the low flows, but our combined model approach has a better representation for small to medium events (also see Fig. S5 for the entire calibration and evaluation periods). The simulation of our combined model approach shows improvement for the discharge recessions at Austrian and Irish sites. Whereas, the traditional non-karstic model is not sensitive to small events and low flows at Irish site. However, few events are underestimated at Austrian site (Fig. S5 at AT) by our combined model approach. This is probably due to the underestimation of surface runoff. The karstic model in our combined model approach has a bigger water storage capacity and infiltration rate, which reduces the possibility for generation of surface runoff. At Israeli site, the two approaches perform similarly regarding the hydrograph simulations.

From calibration to evaluation, our combined model approach has smaller decrease in the predictive skill (slight increase in RMSE and |1-VCC|) compared to the non-karstic model at Austrian and Israeli sites. At the German, French, and Irish sites, the predictive ability of our combined approach does not decrease and is better compared to the non-karstic model. At the Spanish site, the performance of both approaches decrease during the evaluation period. Generally, our combined model approach works equally or better

299 for the stream hydrograph simulations, especially for catchments identified to be influenced by IGF. The
300 comparison between the two approaches confirms the validity of IGF identification by signatures.

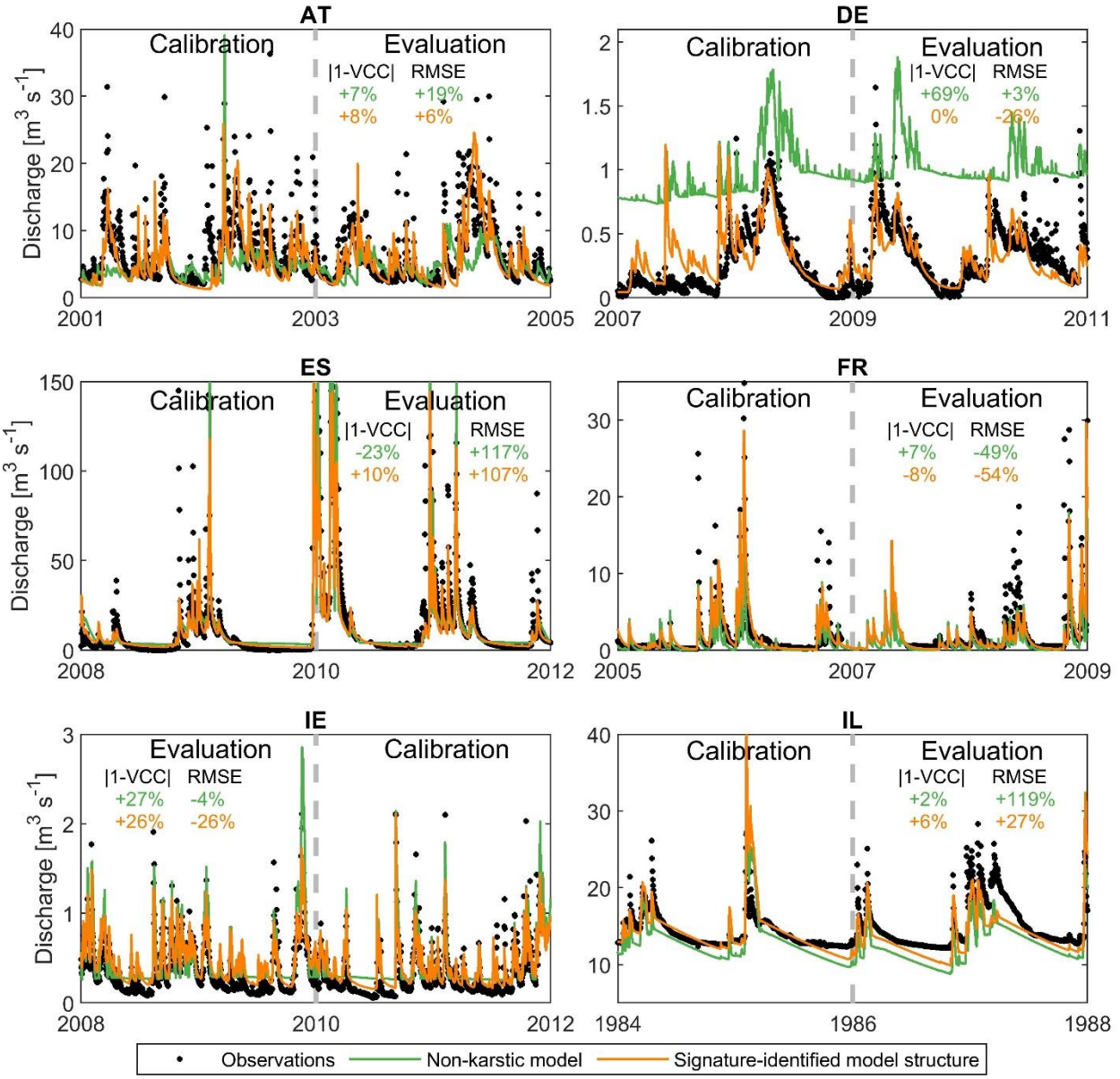

301

302 Figure 4. Visualization of discharge simulations between the two approaches (the non-karstic model VS
303 the signature-identified model structure) at six test catchments. We choose two years of calibration and
304 two years of evaluation to demonstrate some details of the hydrograph. Hydrographs of calibration and
305 evaluation for the entire period are provided in Fig. S5. The term |1-VCC| indicates the distance to the
306 perfect water balance. In each subplot, we provide the percentage change of |1-VCC| and RMSE from the
307 calibration to the evaluation, the smaller and more negative of the two values, the better the predictive
308 skill is.

3.2.2 Verification of model structure selection

The signature-identified model structure outperforms the non-karstic model in terms of water balance (Fig. 5a) and model simulation error (Fig. 5b) at all test sites. We see a similar or equal performance in evaluation period except the Spanish site due to the coarse and less spring discharge observations for calibration. This indicates the validity of our signature-identified model structure. The model including all processes does not improve the model simulation compared to the signature-identified model structure, showing that the signature-based approach provides a good way to identify the appropriate model structure.

Comparing all model structures (Fig. S6), we find that adding the snow process to Austrian and Israeli sites (suggested by the snowfall fraction) improves the model performance (indicated by RMSE). However, adding the channel process to the Israeli site (suggested by the channel length) does not improve the model simulation, which indicates a negligible influence of the Muskingum-Cunge channel process on discharge simulation. Adding karstic process accounting for IGF at the Austrian, German, Spanish, French, and Irish sites (suggested by runoff ratio and ECI), we see a significant improvement in water balance (VCC, Fig. 5a). The overall performance (RMSE, Fig. 5b) at Austrian, German, French, and Irish sites is better as well. It generally shows the consistency with the signature identification for important model processes.

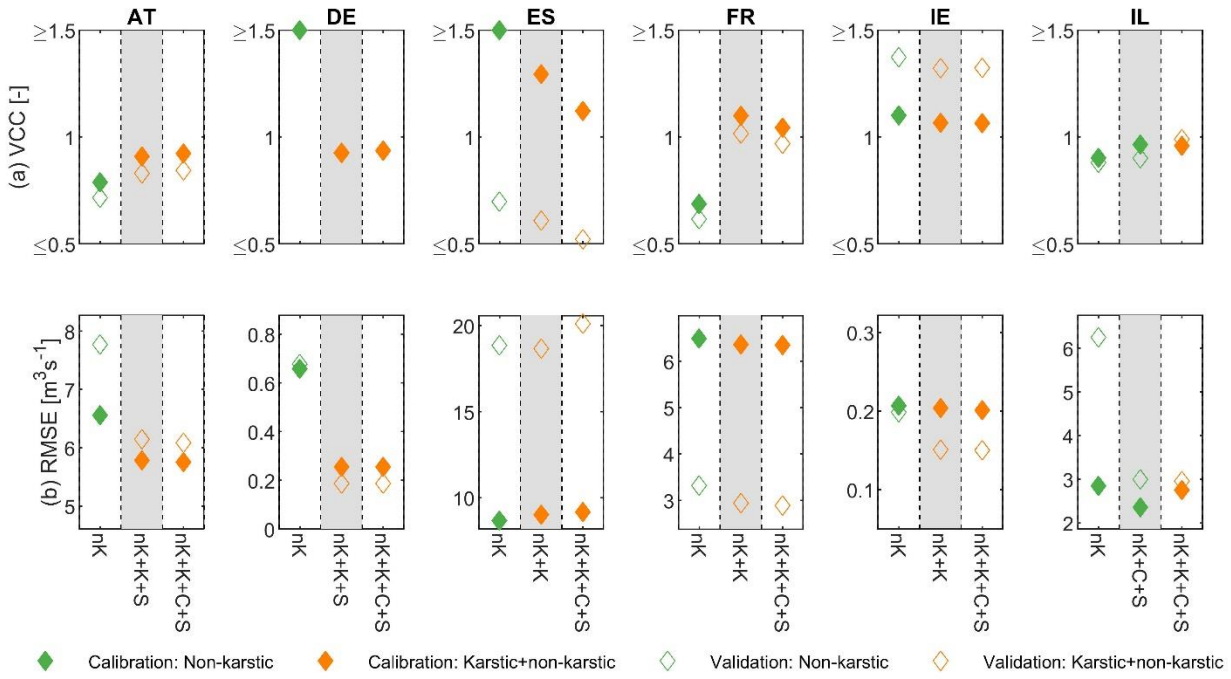

Figure 5. Model performance on (a) the water balance indicated by VCC and (b) the model simulation errors indicated by RMSE. Two approaches are compared: the non-karstic model (in green) VS the combined models accounting for IGF (in orange). We show the performance of three model structures: the non-karstic model without additional processes (nK, the first column in each plot), the selected model structure by signatures (indicated by grey background, the second column in each plot), the model structure with all processes including snow, channel, and karstic process accounting for IGF (nK+K+C+S, the third column in each plot). nK, K, C, and S represent the non-karstic model, karstic model, channel process, and snow process, respectively. The model performance of all model structures (table 3) is provided in Fig. S6.

3.3 Streamflow sensitivity to precipitation variability

Using our combined model approach, we can assess streamflow elasticity of karstic and non-karstic parts of a catchment. At all sites except IL (Fig. 6a), the elasticity of total stream discharge and the specific discharge of karstic and non-karstic parts is all larger than one, suggesting that stream discharge is all sensitive to the precipitation variability no matter the contribution of karstic or non-karstic areas. The elasticity of total stream discharge is affected by the karstic and non-karstic components. But they show site specific characteristics (Fig. 6a). The German, Irish and Israeli sites have similar elasticity of karstic and non-karstic specific discharge. However, the Spanish site has a larger elasticity of the karstic specific discharge than the non-karstic one (Fig. 6a at ES). Due to the typical karst features, the karstic component reacts faster and is more sensitive to the precipitation change at this site. However, we simulate a smaller

elasticity of the karstic specific discharge compared to that of the non-karstic one at the Austrian and French sites. It may be due to high flows; such as surface runoff of the non-karstic area is more sensitive to the precipitation change.

We calculate the elasticity of the total stream discharge under two scenarios, i.e. assuming a closed water balance at the topographic catchment VS our combined model approach considering IGF (Fig. 6b). For the former scenario, the contribution of the karstic component to the total elasticity is mainly controlled by the topographic karst coverage, but also is influenced by the deviation of the elasticity between karstic and non-karstic specific discharge, particularly at the Spanish and French sites. For the latter scenario, the contribution of karst to the total elasticity at German and Irish sites becomes smaller compared to that assuming a closed water balance. Since these two sites have a smaller effective catchment area and lose water through IGF to the neighboring areas. The Spanish and French sites have an increase in the contribution of karst to the total elasticity. As expected, these catchments gain water from neighboring catchments.

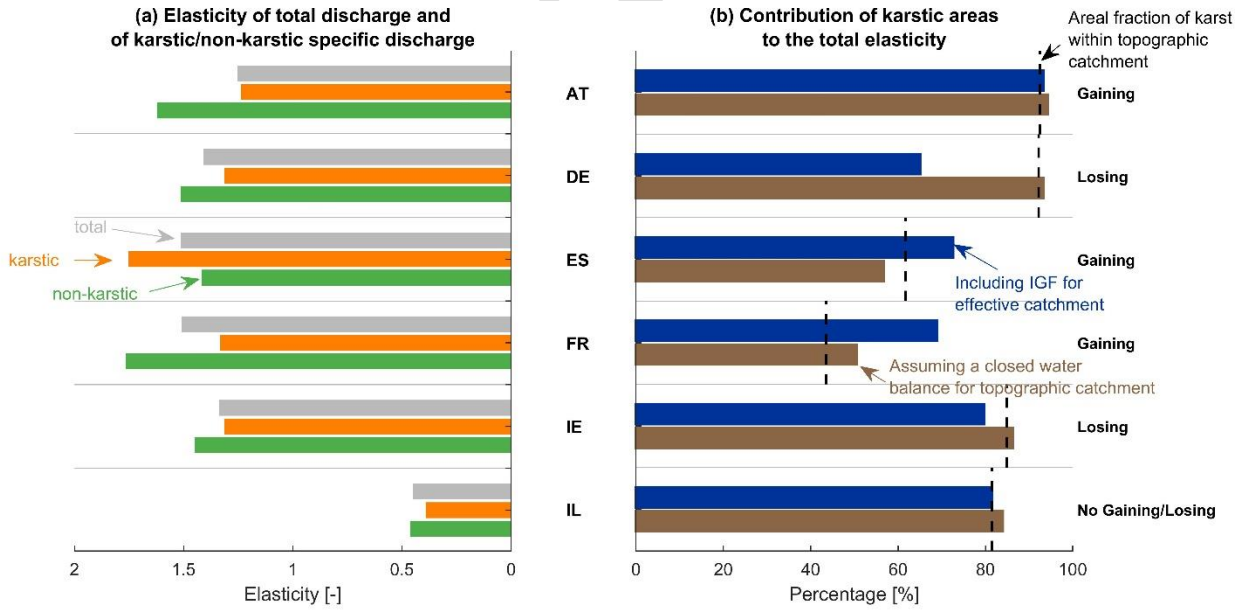

Figure 6. (a) Elasticity of total stream discharge and of karstic/non-karstic specific discharge; and (b) contribution of karstic part to the total discharge sensitivity due to precipitation variability. The calculation is based on the discharge simulations with the selected model structure. We indicate 'Gaining' for catchments that gain water and 'Losing' for catchment that lose water. At IL, there is no obvious IGF, thus gaining and losing is absent.

4 Discussion

4.1 Reliability of the signature-based model structure identification

The non-karstic model fails the simulation of water balance for catchments where IGF is identified to be important (Fig. 5a). As expected, considering IGF at all the sites except IL (suggested by runoff ratio and ECI), we see the general improvement of model simulations. In particular, the water balance is obviously improved (Fig. 5a). Furthermore, parameters representing karstic processes (Fig. S1) as well as the parameter representing IGF (Fig. S4) are identifiable and sensitive according to their posterior distributions derived from $DREAM_{(ZS)}$. This is consistent with the findings of Bouaziz et al (2018) and Le Mesnil et al (2020), who reported the deterioration of catchment water balance due to water gains or losses. One would argue that the signature-identified model structure adding additional processes may over-represent the system response in calibration. In this case, the overfitting will lead to a deterioration from calibration to evaluation, which is not seen in our study.

The snowfall fraction indicates the importance of snow processes for Austrian, German, and Israeli sites. Indeed, the increased performance measured by RMSE is simulated after adding the snow routine, especially at Austrian and Israeli sites (Fig. 5b and Fig. S6b). Parameters regarding snow accumulation and melting at these sites are also identifiable (Fig. S3). This is because the snow accumulation and melting affect the dynamic of water storage and the timing of runoff particularly in winter seasons (Freudiger et al., 2017; Zeinivand & Smedt, 2009). At the German site, the inter-catchment groundwater flow has the dominant influence (Fig. 4 at DE) such that the effect of snow processes is relatively less important.

Adding the channel routing to the Israeli site (suggested by channel length), we do not see obvious improvement of discharge simulation (Fig. S6). Channel processes are important for flood propagation at finer temporal resolution (O'Sullivan et al., 2012). However, the influence of the Muskingum-Cunge channel routine is limited on discharge simulations of the lumped model at the scale of several hundreds

of squared kilometers with daily resolution. More complicated channel methods (usually with more parameters) may also not be necessary for the purpose of daily simulations at small scales.

Compared to the model structure identified by signatures, the model including all processes does not obviously improve the discharge simulation. This model structure introduces 2−6 more parameters for different sites. The parameter controlling the travel time in the channel is not sensitive at almost all the sites (Fig. S4). Snow accumulation and melting parameters are also not identifiable at ES, FR and IE where snow processes are suggested to be irrelevant by snowfall fraction (Fig. S4). This implies that the model structure with all processes introduces more uncertainty and equifinality. Adding additionally unimportant processes increases parameter uncertainty and leads to over-parameterization (Beven, 2006; Schoups et al., 2008). In this case, system signatures help to reduce the unimportant processes such that the equifinality becomes less.

With the split-sample test for the calibration and evaluation, our signature-based approach performs well from calibration to evaluation. In addition, the verification of the important process identification using additional signatures (Fig. S7) denotes a good performance of our signature-based approach. Together with multi-objectives that measure the water balance and model error, we show that multi-objectives and additional signature verification help to identify most appropriate model structures (Gunkel et al., 2015; Wagener et al., 2001). Generally, our analysis indicates that the signature-based model identification provides acceptable estimates of important processes concerning snow and inter-catchment groundwater flow.

4.2 Merits of including karstic processes in catchment-scale modeling

Inclusion of karstic processes in catchment-scale modeling enables the consideration of IGF for catchments partially covered by karst. In particular, the system signature ECI quantifies the water gains or losses via IGF. This approach results in a better representation of catchment-scale water balance, such as solving problems of discharge underestimation at gaining catchments (AT and FR), and of discharge

overestimation at losing catchments (DE and IE). Our approach is also capable to simulate the dynamics of water gains and losses such that we have a better simulation of the catchment hydrodynamics.

Muñoz et al (2016) and Pellicer-Martínez & Martínez-Paz (2014) simulated IGF between neibouring catchments. They require good knowledge of subsurface connectivity, the strength and direction of water gains/losses between donor and receiving catchments. Compared to these studies, our approach requires less spatial and hydrogeological information. Our approach can be easily applied to a topographic catchment without knowing their neighbours. However, the shortcoming is that we only quantify the net IGF with no indication in the direction of water gains/losses. Our approach captures the temporal variation of IGF compared to studies relying on annual water-balance (Le Mesnil et al., 2020). Bouaziz et al (2018) used the Budyko framework to identify IGF; Le Moine et al (2007) used a model parameter to represent the significance of IGF, while our approach uses the newly defined signature ECI (Liu et al., 2020) to quantify IGF. Incorporating IGF to hydrological models, these three approaches are capable to model the influence of IGF on catchment hydrodynamics. The advantage of our approach is that we use karst spring discharge observations to better represent the karstic parts of the catchment and to estimate the water gains/losses through the karstic aquifer.

4.3 Impacts of karst on the streamflow sensitivity to precipitation variability

Schaake (1990), Sankarasubramanian et al (2001) and Vano et al (2012) used precipitation elasticity of streamflow as a measure for the sensitivity of streamflow to changes in precipitation at the catchment scale. Hartmann et al (2013) used elasticity of spring discharge to characterize the inter-annual memory effect of karst spring systems at the karstic aquifer scale. However, it is rarely reported for separating the streamflow sensitivity to karstic and non-karstic parts. Our combined model approach with ECI and karst spring discharge enables us to estimate contributions of the karstic and non-karstic areas to the total streamflow, and thus to separate the streamflow sensitivity to the karstic and non-karstic parts for a catchment partially covered by karst (Fig. 6). Hellwig et al (2020) reported a delayed response from climate extremes to discharge extremes due to diverse delayed response of groundwater to precipitation.

Differentiating the streamflow sensitivity of karstic and non-karstic parts is useful to investigate the system responses under climate extremes, such as drought (Fiorillo, 2009). But in karstic regions, how do karst and IGF influence the system response under climate extremes? Will IGF enhance or reduce the strength of hydrological extremes? These are open questions and need further studies in the future.

Our study shows that the assumptions of catchment water balance affect the estimation of streamflow sensitivity of karstic and non-karstic parts. IGF alters the contribution of the karstic part to the total streamflow sensitivity compared to that assuming a commonly closed water balance at the topographic catchment. The losing catchments have a decreased karstic contribution to the total sensitivity, while an increased karstic contribution is simulated for gaining catchments. The water gains and losses from karst to neighboring areas highlight the importance of karst to the water management. The water management should not only focus on a single catchment, but also need to consider the influence of the cross catchment strategies to include the IGF effects. Our approach provides clues for the possible application of different water management strategies between the karstic and non-karstic areas.

4.4 Transferability of our approach

We identify important processes using signatures and combine karstic and non-karstic processes for karst-influenced catchments. Our approach performs well for six test catchments that cover different climates and landscapes with varying catchment areas and karst coverage. The approach is model-independent, meaning that the karstic and non-karstic models can be replaced by any other hydrological model if found to be more adequate for the envisaged purpose. Thus, this approach can be easily transferred to catchments with similar conditions that are partially covered by karst. Here, we detected karst-influenced catchments using a catchment attribute database (Beck et al., 2019), a karst aquifer map (Chen et al., 2017), and a lithological map (Hartmann & Moosdorf, 2012). Since our approach includes karst spring discharge information to represent the karstic part of a catchment, the karst spring discharge database (Olarinoye et al., 2020) provided additional information on karst spring hydrographs.

Regional and large-scale hydrological models (van Beek & Bierkens, 2008; Döll et al., 2003) have been used for water resources management. However, karst features are not adequately included in such models. Our approach provides a feasible way to incorporate karstic processes in these models based on large-scale recharge simulations in karstic regions (Hartmann et al., 2015). Our approach can be used to evaluate the simulation of karstic contributions to streamflow. Liu et al (2020) showed that a large portion of catchments beyond karst are also influenced by IGF. Similarly to our approach, introducing an additional process (Bouaziz et al., 2018) to account for IGF is crucial to close water balance at the catchment scale. Therefore, considering IGF in large scale modeling may also improve the large scale simulation of groundwater-surface water exchanges (Liu et al., 2020). Furthermore, linking our approach with soil moisture and discharge observation networks (Hartmann et al., 2020) can provide a good basis for better integrated water resources management.

5 Conclusions

In this study, we propose a signature-based approach to identify the most appropriate model structure for karst-influenced catchments with unclosed water balance. We show the validity and reliability of this approach at six test catchments with varying climates and karst coverage. The snowfall fraction is a good indicator to reflect the importance of the snow process, while the channel process is suggested to be unimportant for small catchments with typical daily temporal resolution. The newly introduced signature, effective catchment index (ECI), can provide quantitative estimates of IGF for the streamflow simulation. We combine the karstic and non-karstic processes to include IGF effects in the catchment-scale hydrological modeling for catchments identified with water gains/losses. Our combined model approach performs well for stream discharge simulations, especially improves the water balance significantly for those catchments with IGF influence. This approach enables us to separate the total streamflow to karstic and non-karstic contributions. Therefore, the investigation of the discharge sensitivity of karstic and non-karstic parts becomes possible. IGF reduces the contribution of karst to the total sensitivity for catchments losing water, while increases that for catchments gaining water. Our study provides a feasible way to

combine the karstic and non-karstic processes at the catchment scale and enables the investigation of streamflow sensitivity of karstic and non-karstic domains within the same catchment. It provides a basis of addressing IGF for the hydrological modeling at karst-influenced catchments. It highlights that management strategies should consider IGF influence at karstic regions where flow crossing topographic catchment boundaries often occurs.

Acknowledgement

YL and AH were supported by the Emmy-Noether-Programme of the German Research Foundation (DFG, grant number: HA 8113/1-1; project "Global Assessment of Water Stress in Karst Regions in a Changing World"), TW was partially supported by a Royal Society Wolfson Research Merit Award (WM170042).

Data availability statement

Catchment boundaries are obtained from HydroSHEDS via https://hydrosheds.org/downloads and are confined by DEM obtained from the Copernicus Services via https://land.copernicus.eu/imagery-in-situ/eu-dem/eu-dem-v1.1?tab=download.

Spring discharge is obtained from the WoKaS database described in https://doi.org/10.1038/s41597-019-0346-5

Stream discharge and forcing data of the six test catchments are obtained from public databases of local hydrological services and published articles. The data that is prepared for our modeling can be accessed via https://doi.org/10.5281/zenodo.3987835.

Author contributions

YL, TW and AH conceptualized the paper. YL conducted the model simulations with help of AH. YL, WT and AH performed the analysis. YL wrote the manuscript. WT and AH reviewed and revised the manuscript.

Reference

Bakalowicz, M. (2005). Karst groundwater: A challenge for new resources. *Hydrogeology Journal*, *13*(1), 148–160. https://doi.org/10.1007/s10040-004-0402-9

Beck, H. E., Wood, E. F., McVicar, T. R., Zambrano-Bigiarini, M., Alvarez-Garreton, C., Baez-Villanueva, O. M., et al. (2019). Bias correction of global high-resolution precipitation climatologies using streamflow observations from 9372 catchments. *Journal of Climate*, *33*, 1299–1315. https://doi.org/10.1175/JCLI-D-19-0332.1

van Beek, L., & Bierkens, M. (2008). *The global hydrological model PCR-GLOBWB: conceptualization, parameterization and verification*. Utrecht, The Netherlands. Retrieved from http://vanbeek.geo.uu.nl/suppinfo/vanbeekbierkens2009.pdf

Berthelin, R., Rinderer, M., Andreo, B., Baker, A., Kilian, D., Leonhardt, G., et al. (2020). A soil moisture monitoring network to characterize karstic recharge and evapotranspiration at five representative sites across the globe. *Geoscientific Instrumentation, Methods and Data Systems*, *9*(1), 11–23. https://doi.org/10.5194/gi-9-11-2020

Beven, K. (2006). A manifesto for the equifinality thesis. *Journal of Hydrology*, *320*(1–2), 18–36. https://doi.org/10.1016/j.jhydrol.2005.07.007

Bouaziz, L., Weerts, A., Schellekens, J., Sprokkereef, E., Stam, J., Savenije, H., & Hrachowitz, M. (2018). Redressing the balance: Quantifying net intercatchment groundwater flows. *Hydrology and Earth System Sciences*, *22*(12), 6415–6434. https://doi.org/10.5194/hess-22-6415-2018

Butscher, C., Auckenthaler, A., Scheidler, S., & Huggenberger, P. (2011). Validation of a Numerical Indicator of Microbial Contamination for Karst Springs. *Ground Water*, *49*(1), 66–76. https://doi.org/10.1111/j.1745-6584.2010.00687.x

Chen, Z., Auler, A. S., Bakalowicz, M., Drew, D., Griger, F., Hartmann, J., et al. (2017). The World Karst Aquifer Mapping project: concept, mapping. *Hydrogeology Journal*, *25*(3), 771–785. https://doi.org/10.1007/s10040-016-1519-3

Chen, Z., Hartmann, A., Wagener, T., & Goldscheider, N. (2018). Dynamics of water fluxes and storages in an Alpine karst catchment under current and potential future climate conditions. *Hydrology and Earth System Sciences*, *22*(7), 3807–3823. https://doi.org/10.5194/hess-22-3807-2018

Christensen, J. H., Hewitson, B., Busuioc, A., Chen, A., Gao, X., Held, I., et al. (2007). Regional Climate Projections. The Physical Science Basis. Contribution of Working Group I to the Fourth Assessment Report of the Intergovernmental Panel on Climate Change. Cambridge, UK and New York, NY, USA: Cambridge University Press.

Clark, M. P., Bierkens, M. F. P., Samaniego, L., Woods, R. A., Uijlenhoet, R., Bennett, K. E., et al. (2017). The evolution of process-based hydrologic models: Historical challenges and the collective quest for physical realism. *Hydrology and Earth System Sciences*, *21*(7), 3427–3440. https://doi.org/10.5194/hess-21-3427-2017

Cunge, J. A. (1969). On the subject of a flood propagation computation method (Musklngum method). *Journal of Hydraulic Research*, *7*(2), 205–230.

Döll, P., Kaspar, F., & Lehner, B. (2003). A global hydrological model for deriving water availability indicators: Model tuning and validation. *Journal of Hydrology*, *270*(1–2), 105–134. https://doi.org/10.1016/S0022-1694(02)00283-4

Fan, Y. (2019). Are catchments leaky? *WIREs Water*, *6*(6), e1386. https://doi.org/10.1002/wat2.1386

Fiorillo, F. (2009). Spring hydrographs as indicators of droughts in a karst environment. *Journal of Hydrology*, *373*(3–4), 290–301. https://doi.org/10.1016/j.jhydrol.2009.04.034

Ford, D., & Williams, P. (2007). *Karst Hydrogeology and Geomorphology*. West Sussex, England: John

Wiley & Sons Ltd,. https://doi.org/10.1002/9781118684986

Freudiger, D., Kohn, I., Seibert, J., Stahl, K., & Weiler, M. (2017). Snow redistribution for the hydrological modeling of alpine catchments. *Wiley Interdisciplinary Reviews: Water*, *4*(5), e1232. https://doi.org/10.1002/wat2.1232

Gunkel, A., Shadeed, S., Hartmann, A., Wagener, T., & Lange, J. (2015). Model signatures and aridity indices enhance the accuracy of water balance estimations in a data-scarce Eastern Mediterranean catchment. *Journal of Hydrology: Regional Studies*, *4*, 487–501. https://doi.org/10.1016/j.ejrh.2015.08.002

Hartmann, A., & Baker, A. (2017). Modelling karst vadose zone hydrology and its relevance for paleoclimate reconstruction. *Earth-Science Reviews*, *172*(December 2016), 178–192. https://doi.org/10.1016/j.earscirev.2017.08.001

Hartmann, A., Weiler, M., Wagener, T., Lange, J., Kralik, M., Humer, F., et al. (2013). Process-based karst modelling to relate hydrodynamic and hydrochemical characteristics to system properties. *Hydrology and Earth System Sciences*, *17*(8), 3505–3521. https://doi.org/10.5194/hess-17-3305-2013

Hartmann, A., Barberá, J. A., Lange, J., Andreo, B., & Weiler, M. (2013). Progress in the hydrologic simulation of time variant recharge areas of karst systems – Exemplified at a karst spring in Southern Spain. *Advances in Water Resources*, *54*, 149–160. https://doi.org/10.1016/j.advwatres.2013.01.010

Hartmann, A., Wagener, T., Rimmer, A., Lange, J., Brielmann, H., & Weiler, M. (2013). Testing the realism of model structures to identify karst system processes using water quality and quantity signatures. *Water Resources Research*, *49*(6), 3345–3358. https://doi.org/10.1002/wrcr.20229

Hartmann, A., Goldscheider, N., Wagener, T., Lange, J., & Weiler, M. (2014). Karst water resources in a changing world: Review of hydrological modeling approaches. *Reviews of Geophysics*, *52*(3), 218–242. https://doi.org/10.1002/2013RG000443

Hartmann, A., Gleeson, T., Rosolem, R., Pianosi, F., Wada, Y., & Wagener, T. (2015). A large-scale simulation model to assess karstic groundwater recharge over Europe and the Mediterranean. *Geoscientific Model Development*, *8*(6), 1729–1746. https://doi.org/10.5194/gmd-8-1729-2015

Hartmann, A., Liu, Y., Olarinoye, T., Berthelin, R., & Marx, V. (2020). Integrating field work , large sample hydrology and modeling to inform (inter) national governance of karst water resources. *EarthArXiv*, 1–24. https://doi.org/10.31223/osf.io/8cde3

Hartmann, J., & Moosdorf, N. (2012). The new global lithological map database GLiM: A representation of rock properties at the Earth surface. *Geochemistry, Geophysics, Geosystems*, *13*(12), Q12004. https://doi.org/10.1029/2012GC004370

Haslinger, K., Koffler, D., Schöner, W., & Laaha, G. (2014). Exploring the link between meteorological drought and streamflow: Effects of climate-catchment interaction. *Water Resources Research*, *50*(3), 2468–2487. https://doi.org/10.1002/2013WR015051

Hellwig, J., Graaf, I. E. M., Weiler, M., & Stahl, K. (2020). Large-Scale Assessment of Delayed Groundwater Responses to Drought. *Water Resources Research*, *56*(2), e2019WR025441. https://doi.org/10.1029/2019WR025441

Hingray, B., Schaefli, B., Mezghani, A., & Hamdi, Y. (2010). Signature-based model calibration for hydrological prediction in mesoscale Alpine catchments. *Hydrological Sciences Journal*, *55*(6), 1002–1016. https://doi.org/10.1080/02626667.2010.505572

599 Jourde, H., Lafare, A., Mazzilli, N., Belaud, G., Neppel, L., Dörfliger, N., & Cernesson, F. (2014). Flash
600 flood mitigation as a positive consequence of anthropogenic forcing on the groundwater resource in
601 a karst catchment. *Environmental Earth Sciences*, *71*(2), 573–583. https://doi.org/10.1007/s12665-
602 013-2678-3

603 Kim, N. W., & Lee, J. (2010). Enhancement of the channel routing module in SWAT. *Hydrological*
604 *Processes*, *24*, 96–107. https://doi.org/10.1002/hyp.7474

605 Kirchner, J. W. (2009). Catchments as simple dynamical systems: Catchment characterization, rainfall-
606 runoff modeling, and doing hydrology backward. *Water Resources Research*, *45*(2), W02429.
607 https://doi.org/10.1029/2008WR006912

608 Klemeš, V. (1986). Dilettantism in hydrology: Transition or destiny? *Water Resources Research*, *22*(9S),
609 177S-188S. https://doi.org/10.1029/WR022i09Sp0177S

610 Lehner, B., Verdin, K., & Jarvis, A. (2008). New Global Hydrography Derived From Spaceborne
611 Elevation Data. *Eos, Transactions American Geophysical Union*, *89*(10), 93.
612 https://doi.org/10.1029/2008EO100001

613 Lindström, G., Johansson, B., Persson, M., Gardelin, M., & Bergström, S. (1997). Development and test
614 of the distributed HBV-96 hydrological model. *Journal of Hydrology*, *201*(1–4), 272–288.
615 https://doi.org/10.1016/S0022-1694(97)00041-3

616 Liu, Y., Zarfl, C., Basu, N. B., & Cirpka, O. A. (2020). Modeling the Fate of Pharmaceuticals in a Fourth-
617 Order River Under Competing Assumptions of Transient Storage. *Water Resources Research*, *56*(3),
618 e2019WR026100. https://doi.org/10.1029/2019WR026100

619 Liu, Y, Zarfl, C., Basu, N. B., Schwientek, M., & Cirpka, O. A. (2018). Contributions of catchment and
620 in-stream processes to suspended sediment transport in a dominantly groundwater-fed catchment.
621 *Hydrology and Earth System Sciences*, *22*(7), 3903–3921. https://doi.org/10.5194/hess-22-3903-
622 2018

623 Liu, Y, Wagener, T., Beck, H. E., & Hartmann, A. (2020). What is the hydrologically effective area of a
624 catchment? *Environmental Research Letters*, 1–27. https://doi.org/10.1088/1748-9326/aba7e5

625 Liu, Yan, Zarfl, C., Basu, N. B., & Cirpka, O. A. (2019). Turnover and legacy of sediment-associated
626 PAH in a baseflow-dominated river. *Science of The Total Environment*, *671*, 754–764.
627 https://doi.org/10.1016/j.scitotenv.2019.03.236

628 Lüthi, M. P. (2019). Stream Gauge Calibration of a Cave Stream Using Water Temperature Variability as
629 a Tracer. *Water Resources Research*, *55*(7), 5738–5750. https://doi.org/10.1029/2018WR023762

630 Martens, B., Miralles, D. G., Lievens, H., Van Der Schalie, R., de Jeu, R. A. M., Fernández-Prieto, D., et
631 al. (2017). GLEAM v3: Satellite-based land evaporation and root-zone soil moisture. *Geoscientific*
632 *Model Development*, *10*(5), 1903–1925. https://doi.org/10.5194/gmd-10-1903-2017

633 McMillan, H. K., Westerberg, I. K., & Krueger, T. (2018). Hydrological data uncertainty and its
634 implications. *WIREs Water*, *5*(6), 1–14. https://doi.org/10.1002/wat2.1319

635 Merz, R., & Blöschl, G. (2005). Flood frequency regionalisation - Spatial proximity vs. catchment
636 attributes. *Journal of Hydrology*, *302*(1–4), 283–306. https://doi.org/10.1016/j.jhydrol.2004.07.018

637 Le Mesnil, M., Charlier, J.-B., Moussa, R., Caballero, Y., & Dörfliger, N. (2020). Interbasin groundwater
638 flow: Characterization, role of karst areas, impact on annual water balance and flood processes.
639 *Journal of Hydrology*, *585*, 124583. https://doi.org/10.1016/j.jhydrol.2020.124583

Van Meter, K. J., & Basu, N. B. (2017). Time lags in watershed-scale nutrient transport: An exploration of dominant controls. *Environmental Research Letters*, *12*(8). https://doi.org/10.1088/1748-9326/aa7bf4

Miralles, D. G., Holmes, T. R. H., De Jeu, R. A. M., Gash, J. H., Meesters, A. G. C. A., & Dolman, A. J. (2011). Global land-surface evaporation estimated from satellite-based observations. *Hydrology and Earth System Sciences*, *15*(2), 453–469. https://doi.org/10.5194/hess-15-453-2011

Miralles, D. G., Jiménez, C., Jung, M., Michel, D., Ershadi, A., Mccabe, M. F., et al. (2016). The WACMOS-ET project - Part 2: Evaluation of global terrestrial evaporation data sets. *Hydrology and Earth System Sciences*, *20*(2), 823–842. https://doi.org/10.5194/hess-20-823-2016

Le Moine, N., Andréassian, V., Perrin, C., & Michel, C. (2007). How can rainfall-runoff models handle intercatchment groundwater flows? Theoretical study based on 1040 French catchments. *Water Resources Research*, *43*(6), W06428. https://doi.org/10.1029/2006WR005608

Morales, T., Fdez. de Valderrama, I., Uriarte, J. A., Antigüedad, I., & Olazar, M. (2007). Predicting travel times and transport characterization in karst conduits by analyzing tracer-breakthrough curves. *Journal of Hydrology*, *334*(1–2), 183–198. https://doi.org/10.1016/j.jhydrol.2006.10.006

Mudarra, M., Hartmann, A., & Andreo, B. (2019). Combining Experimental Methods and Modeling to Quantify the Complex Recharge Behavior of Karst Aquifers. *Water Resources Research*, *55*(2), 1384–1404. https://doi.org/10.1029/2017WR021819

Muñoz, E., Arumí, J. L., Wagener, T., Oyarzún, R., & Parra, V. (2016). Unraveling complex hydrogeological processes in Andean basins in south-central Chile: An integrated assessment to understand hydrological dissimilarity. *Hydrological Processes*, *30*(26), 4934–4943. https://doi.org/10.1002/hyp.11032

O'Sullivan, J. J., Ahilan, S., & Bruen, M. (2012). A modified Muskingum routing approach for floodplain flows: Theory and practice. *Journal of Hydrology*, *470–471*, 239–254. https://doi.org/10.1016/j.jhydrol.2012.09.007

Olarinoye, T., Gleeson, T., Marx, V., Seeger, S., Adinehvand, R., Allocca, V., et al. (2020). Global karst springs hydrograph dataset for research and management of the world's fastest-flowing groundwater. *Scientific Data*, *7*(1), 59. https://doi.org/10.1038/s41597-019-0346-5

Pellicer-Martínez, F., & Martínez-Paz, J. M. (2014). Assessment of interbasin groundwater flows between catchments using a semi-distributed water balance model. *Journal of Hydrology*, *519*(PB), 1848–1858. https://doi.org/10.1016/j.jhydrol.2014.09.067

Perrin, C., Michel, C., & Andréassian, V. (2001). Does a large number of parameters enhance model performance? Comparative assessment of common catchment model structures on 429 catchments. *Journal of Hydrology*, *242*(3–4), 275–301. https://doi.org/10.1016/S0022-1694(00)00393-0

Perrin, J., & Luetscher, M. (2008). Inference of the structure of karst conduits using quantitative tracer tests and geological information: Example of the Swiss Jura. *Hydrogeology Journal*, *16*(5), 951–967. https://doi.org/10.1007/s10040-008-0281-6

Pinault, J. L., Pauwels, H., & Cann, C. (2001). Inverse modeling of the hydrological and the hydrochemical behavior of hydrosystems: Application to nitrate transport and denitrification. *Water Resources Research*, *37*(8), 2179–2190. https://doi.org/10.1029/2001WR900017

Pronk, M., Goldscheider, N., & Zopfi, J. (2006). Dynamics and interaction of organic carbon, turbidity and bacteria in a karst aquifer system. *Hydrogeology Journal*, *14*(4), 473–484. https://doi.org/10.1007/s10040-005-0454-5

Pullan, S. P., Whelan, M. J., Rettino, J., Filby, K., Eyre, S., & Holman, I. P. (2016). Development and application of a catchment scale pesticide fate and transport model for use in drinking water risk assessment. *Science of the Total Environment*, *563–564*, 434–447. https://doi.org/10.1016/j.scitotenv.2016.04.135

Reimann, T., Geyer, T., Shoemaker, W. B., Liedl, R., & Sauter, M. (2011). Effects of dynamically variable saturation and matrix-conduit coupling of flow in karst aquifers. *Water Resources Research*, *47*(11), W11503. https://doi.org/10.1029/2011WR010446

Rimmer, A., & Salingar, Y. (2006). Modelling precipitation-streamflow processes in karst basin: The case of the Jordan River sources, Israel. *Journal of Hydrology*, *331*(3–4), 524–542. https://doi.org/10.1016/j.jhydrol.2006.06.003

Sankarasubramanian, A., Vogel, R. M., & Limbrunner, J. F. (2001). Climate elasticity of streamflow in the United States. *Water Resources Research*, *37*(6), 1771–1781. https://doi.org/10.1029/2000WR900330

Sawicz, K., Wagener, T., Sivapalan, M., Troch, P. A., & Carrillo, G. (2011). Catchment classification: Empirical analysis of hydrologic similarity based on catchment function in the eastern USA. *Hydrology and Earth System Sciences*, *15*(9), 2895–2911. https://doi.org/10.5194/hess-15-2895-2011

Sawicz, K. A., Kelleher, C., Wagener, T., Troch, P., Sivapalan, M., & Carrillo, G. (2014). Characterizing hydrologic change through catchment classification. *Hydrology and Earth System Sciences*, *18*(1), 273–285. https://doi.org/10.5194/hess-18-273-2014

Schaake, J. C. (1990). From climate to flow. In *Climate change and US water resources.* (pp. 177–206). New York, USA: John Wiley and Sons Inc.

Schoups, G., van de Giesen, N. C., & Savenije, H. H. G. (2008). Model complexity control for hydrologic prediction. *Water Resources Research*, *44*(12), W00B03. https://doi.org/10.1029/2008WR006836

Segond, M. L., Wheater, H. S., & Onof, C. (2007). The significance of spatial rainfall representation for flood runoff estimation: A numerical evaluation based on the Lee catchment, UK. *Journal of Hydrology*, *347*(1–2), 116–131. https://doi.org/10.1016/j.jhydrol.2007.09.040

Sherriff, S. C., Rowan, J. S., Fenton, O., Jordan, P., Melland, A. R., Mellander, P. E., & Huallacháin, D. (2016). Storm Event Suspended Sediment-Discharge Hysteresis and Controls in Agricultural Watersheds: Implications for Watershed Scale Sediment Management. *Environmental Science and Technology*, *50*(4), 1769–1778. https://doi.org/10.1021/acs.est.5b04573

Smiatek, G., Mizyed, N., Kunstmann, H., Vivó Aguado, À., Lange, J., & Hartmann, A. (2012). A multi-model approach for improved simulations of future water availability at a large Eastern Mediterranean karst spring. *Journal of Hydrology*, *468–469*, 130–138. https://doi.org/10.1016/j.jhydrol.2012.08.024

Stevanović, Z. (2019). Karst waters in potable water supply: a global scale overview. *Environmental Earth Sciences*, *78*(23), 662. https://doi.org/10.1007/s12665-019-8670-9

Tallaksen, L. M., Hisdal, H., & Lanen, H. A. J. V. (2009). Space-time modelling of catchment scale drought characteristics. *Journal of Hydrology*, *375*(3–4), 363–372. https://doi.org/10.1016/j.jhydrol.2009.06.032

Vano, J. A., Das, T., & Lettenmaier, D. P. (2012). Hydrologic sensitivities of Colorado River runoff to changes in precipitation and temperature. *Journal of Hydrometeorology*, *13*(3), 932–949. https://doi.org/10.1175/JHM-D-11-069.1

Vrugt, J. A. (2016). Markov chain Monte Carlo simulation using the DREAM software package: Theory, concepts, and MATLAB implementation. *Environmental Modelling and Software*, *75*, 273–316. https://doi.org/10.1016/j.envsoft.2015.08.013

Wagener, T., Boyle, D. P., Lees, M. J., Wheater, H. S., Gupta, H. V., & Sorooshian, S. (2001). A framework for development and application of hydrological models. *Hydrology and Earth System Sciences*, *5*(1), 13–26. https://doi.org/10.5194/hess-5-13-2001

Wagener, T., Sivapalan, M., Troch, P., & Woods, R. (2007). Catchment Classification and Hydrologic Similarity. *Geography Compass*, *1*(4), 901–931. https://doi.org/10.1111/j.1749-8198.2007.00039.x

Weiler, M., Arbel, Y., Lange, J., Greenbaum, N., & Hartmann, A. (2012). A new approach to model the spatial and temporal variability of recharge to karst aquifers. *Hydrology and Earth System Sciences*, *16*(7), 2219–2231. https://doi.org/10.5194/hess-16-2219-2012

Williams, J. R. (1969). Flood Routing With Variable Travel Time or Variable Storage Coefficients. *Transactions of the ASAE*, *12*(1), 0100–0103. https://doi.org/10.13031/2013.38772

Yadav, M., Wagener, T., & Gupta, H. (2007). Regionalization of constraints on expected watershed response behavior for improved predictions in ungauged basins. *Advances in Water Resources*, *30*(8), 1756–1774. https://doi.org/10.1016/j.advwatres.2007.01.005

Zeinivand, H., & Smedt, F. (2009). Hydrological modeling of snow accumulation and melting on river basin scale. *Water Resources Management*, *23*(11), 2271–2287. https://doi.org/10.1007/s11269-008-9381-2

Zuo, D., Xu, Z., Yao, W., Jin, S., Xiao, P., & Ran, D. (2016). Assessing the effects of changes in land use and climate on runoff and sediment yields from a watershed in the Loess Plateau of China. *Science of the Total Environment*, *544*, 238–250. https://doi.org/10.1016/j.scitotenv.2015.11.060